RESEARCH

Sensing of Co²⁺ and Cu²⁺ Ions Using Dimethylamino-functionalized Poly(azomethine-1,3,4-oxadiazole)s

Mihaela Homocianu[1] · Elena Hamciuc[1] · Corneliu Hamciuc[1]

Abstract

The ability of OxT and OxFl azomethines to recognize metal ions in THF solutions was investigated using UV-vis absorption techniques. Various metal ions, including Cd^{2+}, Hg^{2+}, Co^{2+}, Sn^{2+}, Cu^{2+}, Ni^{2+}, Zn^{2+} and Ag^+, were tested. The absorption spectra revealed two distinct π-π* transition bands in the 273–278 nm and 330–346 nm wavelength ranges. Additionally, OxFl displayed an absorption peak at 309 nm, attributed to the fluorene group. Spectral titrations were used to study the fluorescence behavior in the presence of these metal ions. The results showed significant quenching with Co^{2+} and Cu^{2+} ions, while other metal ions had minimal effects on the fluorescence intensity. The quenching mechanism was further analyzed using the Stern-Volmer and Lehrer equations, and the binding constants (K_b^{fl}) were calculated using the Benesi-Hildebrand relations. The results confirm that Co^{2+} has a 1:2 stoichiometry and Cu^{2+} has a 1:1 stoichiometry, indicating the strong affinity of OxFl and OxT for these ions. The negative values of ΔG (Gibbs free energy) suggest that complex formation occurs spontaneously at room temperature.

Keywords Co^{2+} and Cu^{2+} ions · Polyazomethines · Absorption and fluorescence spectroscopy · Sensors

Introduction

Poly(azomethine-1,3,4-oxadiazole) materials have potential applications in organic light-emitting diodes [1, 2], liquid crystals [3], and chemosensors due to their unique properties. These materials contain azomethine moieties that can form coordination bonds with metal ions. Materials containing 1,3,4-oxadiazole groups with N and O atoms are useful for chemosensing applications because they provide potential metal coordination sites.

Poly(azomethine-1,3,4-oxadiazole) materials are excellent for the detection of various cations, including Cu^{2+}, [4, 5] Zn^{2+}, [6] Cd^{2+}, [7] and Ag^+, [8] due to the combination of azomethine and oxadiazole groups. Copper and cobalt ions are abundant transition metals in the human body and are involved in various physiological and biological processes. However, excessive levels of copper can lead to adverse health effects, including Alzheimer's disease, Parkinson's disease, Wilson's disease, and other

pathological conditions [9, 10]. Therefore, it is crucial to detect and monitor these metal ions in real time to protect the environment and ensure human health and safety. According to the World Health Organization (WHO), the maximum levels of copper and cobalt ions in drinking water should not exceed 0.5 to 1 μM, and 31.4 μM, respectively [11, 12]. As a result, there is a growing need for efficient methods to detect and quantify these ions. Several techniques have been reported for detecting Co^{2+} and Cu^{2+} ions, including absorption spectrometry (AAS) [13, 14] inductively coupled plasma mass spectrometry (ICP-MS) [15], electrochemistry [16, 17], chemosensors [18–20], and voltammetry [21]. Optical sensors are the most suitable techniques due to their simplicity, low cost, and ease of use. Photoactive materials containing azomethine and 1,3,4-oxadiazole groups are promising candidates for the detection of metal ions because of their simplicity, low cost, high sensitivity, and ability to enable naked-eye detection. These materials have shown remarkable potential for the detection of Co^{2+} and Cu^{2+} ions. However, few studies have been published on the use of azomethine and 1,3,4-oxadiazole based photoactive materials for this purpose. Karami et al. [22] developed azomethine- AuNPs in an aqueous medium that can detect

✉ Mihaela Homocianu
michalupu@yahoo.co.uk; mlupu@icmpp.ro

[1] "Petru Poni" Institute of Macromolecular Chemistry, 41A, Grigore Ghica Voda Alley, 700487 Iasi, Romania
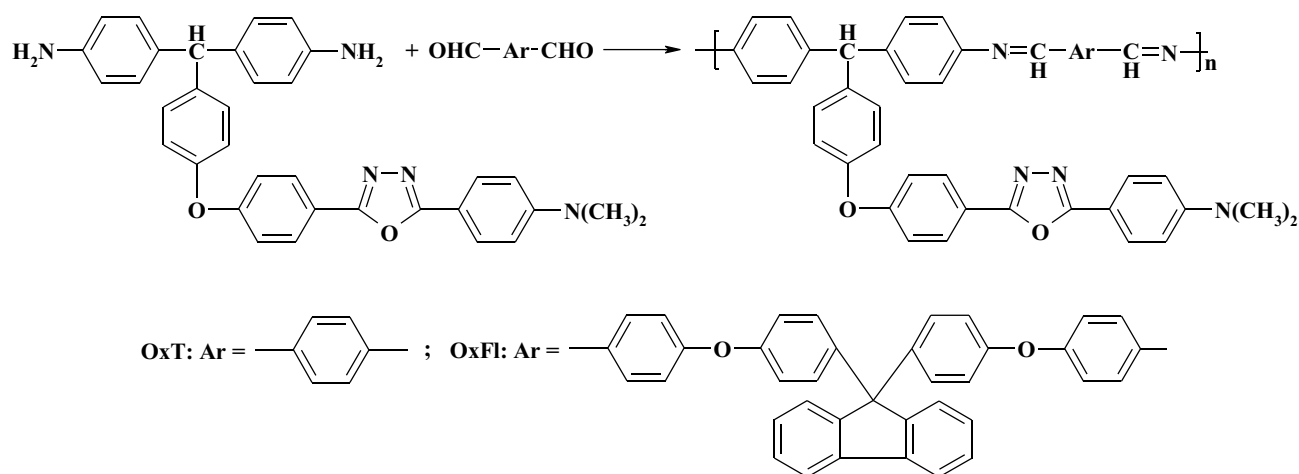
Scheme 1 Molecular structures of OxT and OxFl compounds

copper ions with a detection limit of 83.22 nM. Similarly, Divya and Thennarasu [23] synthesized an indole-pyrazole π-conjugate system for the colorimetric detection of micromolar Co^{2+} concentrations in environmental samples, which could be detected by the naked eye. New derivatives containing 1,3,4-oxadiazole groups have been prepared and used for the precise and sensitive fluorometric detection of Cu^{2+} ions [24, 25].

In our previous study [26], we analyzed the absorption and fluorescence spectral characteristics of OxFl and OxT in tetrahydrofuran (THF), dichloromethane (DCM), N-methyl-2-pyrrolidinone (NMP), and dimethyl sulphoxide (DMSO). The aim of this study was to evaluate the potential of OxFl and OxT as sensors for various metal ions, including Cd^{2+}, Hg^{2+}, Co^{2+}, Sn^{2+}, Cu^{2+}, Ni^{2+}, Zn^{2+}, and Ag^+. UV-Vis absorption and fluorescence titration experiments were performed. The experiments revealed distinct π-π* transition bands and significant fluorescence quenching upon additions of Co^{2+} and Cu^{2+} ions. These observations demonstrate the strong affinities of OxT and OxFl for these metals. The calculated binding constants and Gibbs free energy calculations suggest that the complex formation between these compounds and Co^{2+} and Cu^{2+} ions is spontaneous. These results demonstrate that OxFl and OxT can be used as effective sensors for the detection of Co^{2+} and Cu^{2+} ions in industrial water sources.

Experimental Section

The OxT and OxFl polyazomethines were synthesized through solution polycondensation reactions. The reactions used a diamine and either terephthalic aldehyde or bis(4-formylphenoxyphenyl) fluorine as reactants, while NMP served as solvent [26].

OxT Yield 76%; FTIR (KBr, cm^{-1}): 3040 (aromatic C-H), 2940 and 2880 (aliphatic), 1693 (terminal aldehyde group), 1620 (-CH=N- group), 1240 (aromatic ether linkage), 1019 and 960 (oxadiazole ring), 826 (p-substituted benzene); ^{1}H NMR (400 MHz, CDCl$_3$, ppm): 8.45 (**d**, 2H, J = 8.4 Hz, -CH=N- groups), 8.1–7.7 (**m**, C-H aromatic in ortho- position of -CH=N- units and 1,3,4-oxadiazole rings), 7.5–6.6 (**m**, aromatic), 5.60 (**s**, aliphatic CH of diamine segments), 3.05 (**s**, C-H of methyl from dimethylamino groups) [26].

OxFl Yield 71%; FTIR (KBr, cm^{-1}): 3033 (aromatic C-H), 2930 and 2880 (aliphatic), 1694 (terminal aldehyde group), 1618 (-CH=N- group), 1240 (aromatic ether linkage), 1017 and 958 (oxadiazole ring), 826 (p-substituted benzene); ^{1}H NMR (400 MHz, CDCl$_3$, ppm): 8,56 (**d**, -CH=N- group) s, 8.1–7.8 (**m**, C-H aromatic in ortho- position of -CH=N- units and 1,3,4-oxadiazole rings), 7.6–6.6 (m, aromatic), 5.60 (**s**, aliphatic CH of diamine segments), 3.05 (**s**, C-H of methyl from dimethylamino groups) [26].

The molecular structures of the OxT and OxFl polyazomethines investigated in this study are shown in Scheme 1. To evaluate their sensitivity to various metal ions, including M^{n+} (Cd^{2+}, Hg^{2+}, Co^{2+}, Sn^{2+}, Cu^{2+}, Ni^{2+}, Zn^{2+}, and Ag^+), a series of UV-Vis absorption and fluorescence experiments were performed. Spectral titrations were performed by incrementally adding M^{n+} (0–1500 μL, 10^{-3} M) to 2.5 mL solutions of OxT and OxFl (maintaining the concentration constant) in quartz cuvettes using a Hamilton syringe. Absorption spectra were recorded using a Shimadzu UV 3600 spectrophotometer, whereas fluorescence spectra were measured using a Perkin Elmer LS55 spectrofluorometer. Spectral profiles were recorded for each incremental addition of metal ions. The measurements were performed at room temperature using spectroscopic-grade solvents. The data were analyzed using Origin software.

Results and Discussion

Absorption Spectral Titrations

The ability of OxT and OxFl azomethines to detect Cd^{2+}, Hg^{2+}, Co^{2+}, Sn^{2+}, Cu^{2+}, Ni^{2+}, Zn^{2+}, and Ag^+ was investigated. The interactions between the polyazomethines and metal ions were characterized using UV-vis absorption spectroscopy. Figure 1 shows that both OxT and OxFl exhibit distinct π-π* transition absorption bands in the 273–278 nm and 330–346 nm wavelength regions. The absorption bands result from electronic transitions within the conjugated azomethine

moieties of polyazomethines. The OxFl sample displayed an additional absorption peak at 309 nm, due to the fluorene moiety in the OxFl structure, which introduces a chromophore and affects the overall absorption profile [27].

The addition of metal ions caused significant changes in the absorption spectra of OxT and OxFl polyazomethines. The spectral changes were significant when titrated with increasing amounts of Co^{2+}, Cu^{2+}, Sn^{2+}, and Ni^{2+} ions, showing the sensitivity of the polyazomethines to these metal ions (Fig. 1). In contrast, the presence of Cd^{2+}, Hg^{2+}, Sn^{2+}, Ni^{2+}, Zn^{2+}, and Ag^+ ions decreased the absorption intensity of the band centered at 302 nm for both
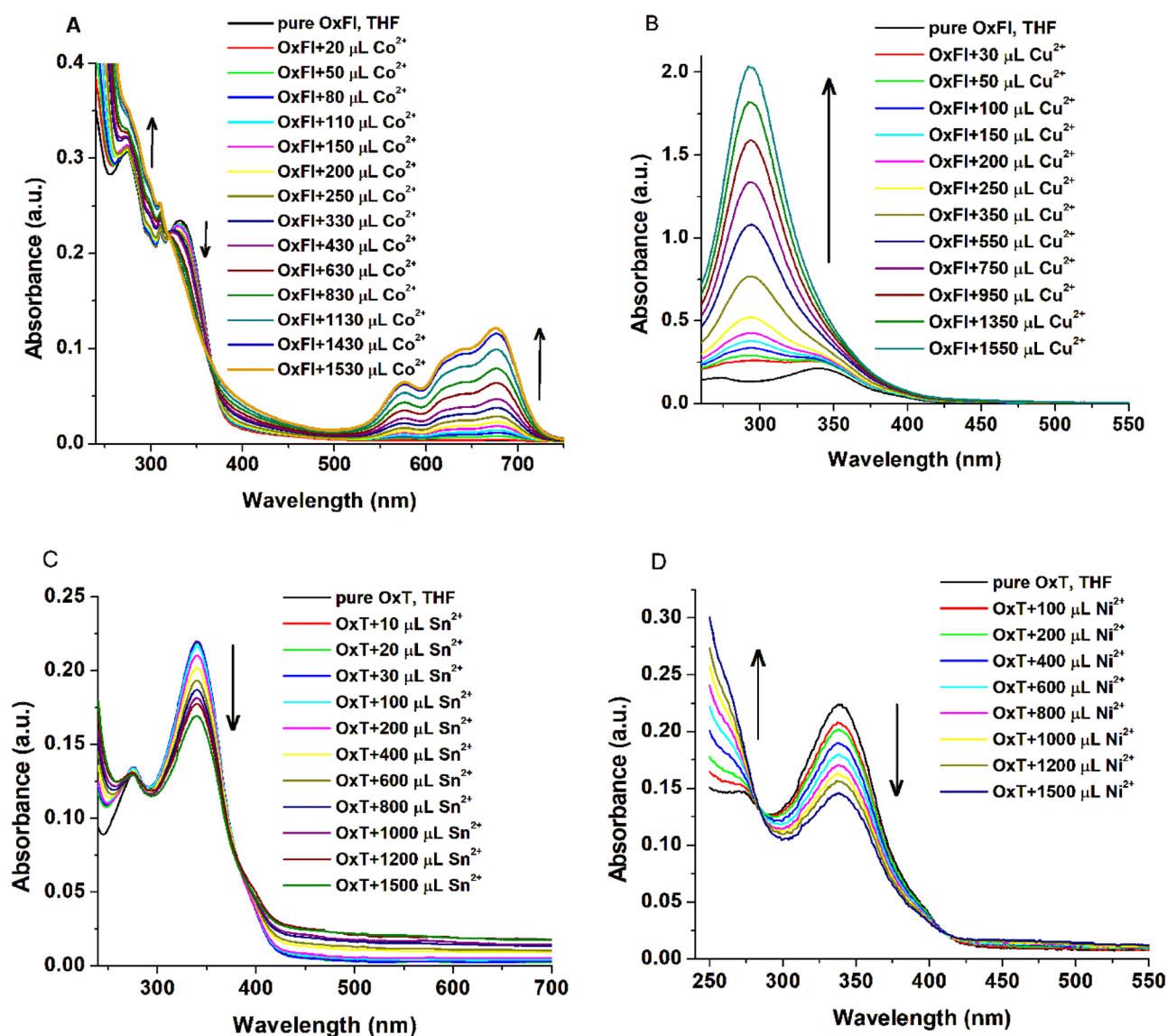

Fig. 1 Absorption spectral changes of OxFl in THF solutions upon the addition of ~1500 μL of Co^{2+} (**A**), Cu^{2+} (**B**), and OxT upon the addition of ~1500 μL of Sn^{2+} (**C**), and Ni^{2+} (**D**) ions. The arrows in the figures indicate the variations in the absorption intensity corresponding to increasing metal ion concentrations

azomethines (Supplementary Figs. S1 and S2). This indicates that the complexation of these metal ions with OxT and OxFl polyazomethines interrupts electronic transitions.

Interestingly, the addition of Cu^{2+} ions to the OxFl sample resulted in increased absorbance, suggesting the formation of a charge transfer complex between OxFl and Cu^{2+} ions. This demonstrates the selective recognition ability of OxFl for Cu^{2+} ions.

Furthermore, the introduction of Co^{2+} ions (Fig. 1A) to the OxFl and OxT solutions resulted in the appearance of a new absorption band with maxima at 676 nm and two additional shoulders at 576 and 632 nm, respectively. The spectral changes exhibited by these azomethines indicate their potential for selective identification and detection of metal ions.

Fluorescence Spectral Titrations

The fluorescence spectra of OxFl and OxT were recorded in THF solutions with varying concentrations of different metal ions, including Cd^{2+}, Hg^{2+}, Co^{2+}, Sn^{2+}, Cu^{2+}, Ni^{2+}, Zn^{2+}, and Ag^{+}. The emission peaks of pure OxFl and OxT were observed at 417 and 419 nm, respectively. Figure 2 shows that the fluorescence intensities of both compounds were significantly quenched upon the addition of 1500 μL of Co^{2+} and Cu^{2+} ions, whereas no significant changes were observed when equivalent amounts of other metal ions, such as Cd^{2+}, Hg^{2+}, Sn^{2+}, Ni^{2+}, Zn^{2+}, and Ag^{+}, were added. These variations in the fluorescence behavior can be attributed to the differences in the electronic properties, ionic radii, and chemical reactivity of Co^{2+} and Cu^{2+} compared to
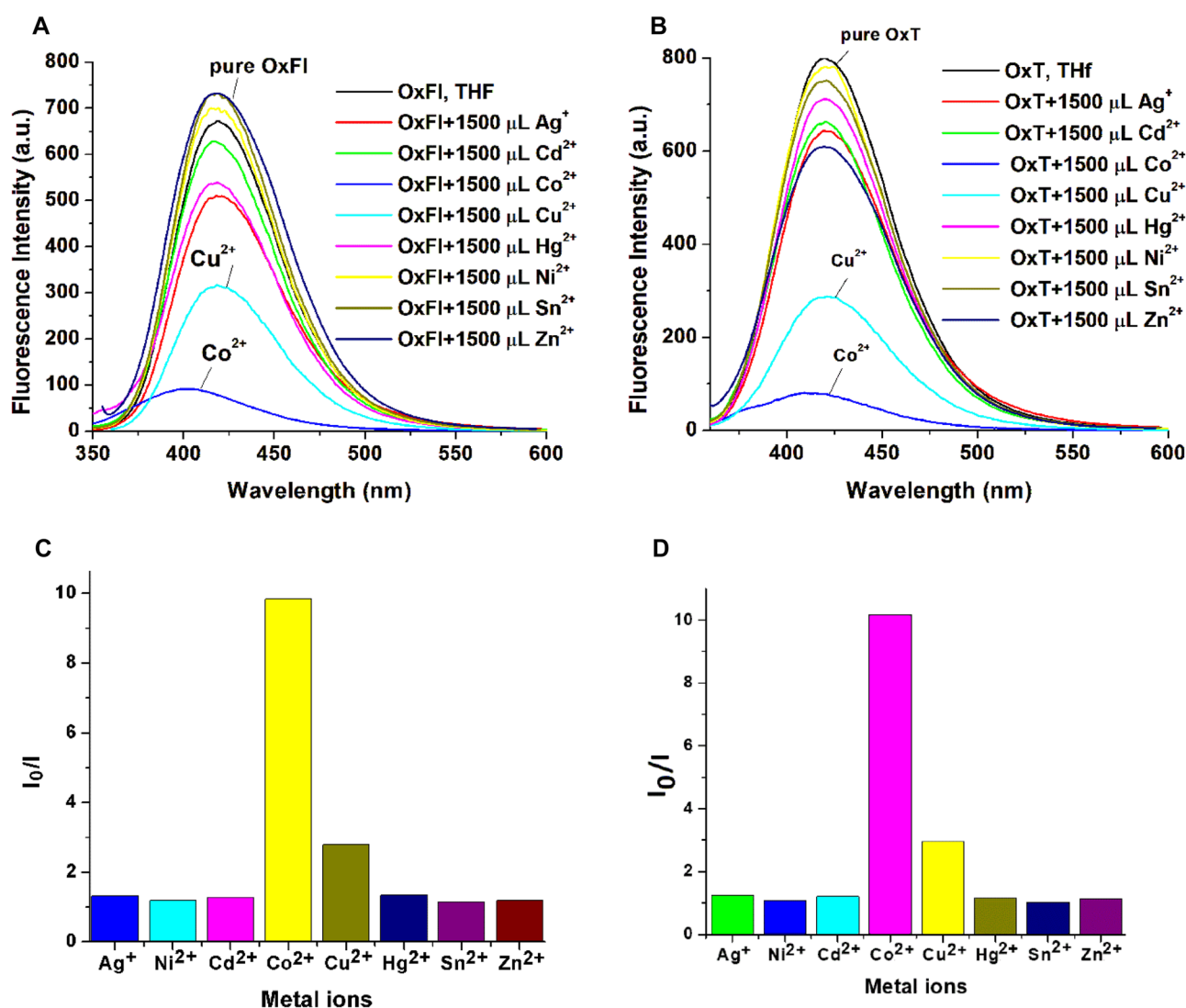

Fig. 2 Fluorescence spectra (excitation wavelength - 300 nm) of pure OxFl (**A**) and OxT (**B**) and bar diagrams of I_0/I for OxFl (**C**) and OxT (**D**) in THF solvent, created after the addition of 1500 μL of each metal ion

the other metal ions tested. The fluorescence intensity of the azomethine derivatives was quenched due to distinct binding modes or electron transfer reactions between Co^{2+} and Cu^{2+} ions and the azomethine moieties in OxFl and OxT. Two bar diagrams (Fig. 2C and D) were created to illustrate the changes in the fluorescence intensity caused by different metal ions. The diagrams show that fluorescence intensity decreases significantly with the addition of Co^{2+} and Cu^{2+}, whereas other metal ions have minimal quenching effects.

A detailed study investigated the effects of Co^{2+} and Cu^{2+} ion titrations on the OxFl and OxT solutions, as depicted in Fig. 3. The fluorescence spectra of pure azomethines in THF displayed intense emission bands, with maxima at

420 and 419 nm. As the concentration of Co^{2+} increased (Fig. 3A), the emission intensity decreased significantly, and the spectral band slightly blue-shifted from 410 to 404 nm, indicating the formation of the OxFl-Co^{2+} complex. However, when titrated with Cu^{2+} ions, the fluorescence intensity decreased without any significant spectral shift. Only Co^{2+} ions induced complete fluorescence quenching in both samples, resulting in an approximately 90% reduction in intensity (Fig. 3A and C). The quenched fluorescence reached a minimum plateau at approximately 1430 μL Co^{2+} for OxFl (Fig. 3A). In contrast, titrations with Cu^{2+} resulted in a fluorescence intensity quenching of approximately 64.16% (Fig. 3B and D). Other tested metal ions, including Cd^{2+},
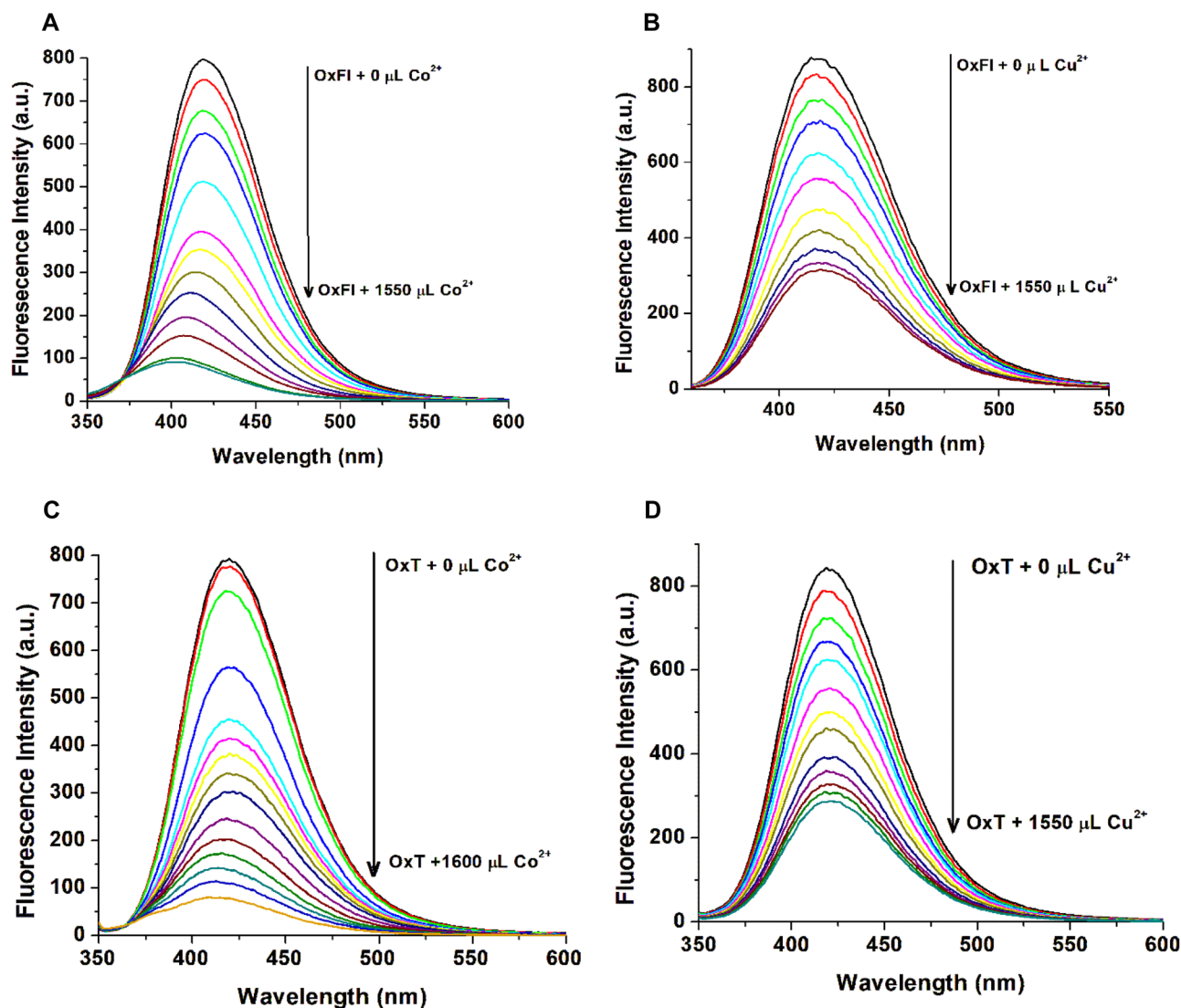

Fig. 3 Spectrofluorometric titrations of OxFl and OxT azomethines (1.07×10^{-3} mol/L, $\lambda_{ex} = 300$ nm, $\lambda_{em} = 417$ nm) in THF solution with Co^{2+} (**A**, **C**) and Cu^{2+} (**B**, **D**) ions. The arrows show variations in emission intensity with increasing metal ion concentration

Hg^{2+}, Sn^{2+}, Ni^{2+}, Zn^{2+}, and Ag^+, had insignificant effects on fluorescence intensity, with the compounds remaining highly fluorescent (quenching percentage (QP %) was approximately 6.61%, as summarized in Table 1). The OxT sample exhibited a similar trend in the presence of Co^{2+} and Cu^{2+} (Fig. 3). These results demonstrate the high selectivity of OxFl and OxT azomethines for Co^{2+} ions.

The limit of detection (LOD) for Co^{2+} and Cu^{2+} ions using OxT and OxFl azomethines was determined based on fluorescence titration data. The LOD was calculated using the following relation: LOD = 3SD/slope. The "slope" was obtained from the linear plot between I_0/I and $[Co^{2+}]$ or $[Cu^{2+}]$ concentrations (Fig. S3), and SD is the standard deviation of the blank signal. Table 1 summarizes the LOD obtained for copper and cobalt ions using OxFl and OxT azomethines. The calculated LOD values for Cu^{2+} using OxFl and OxT were approximately 1.866×10^{-5} and 2.024×10^{-5} M, respectively. These results indicate that the studied azomethines exhibited greater selectivity towards Co^{2+} ions than Cu^{2+}. Literature reports the recognition of Cu^{2+} using different Schiff bases. The detection limits in this context range from $0.6–4.23 \times 10^{-6}$ M [28, 29]. These findings offer valuable insights into the potential applications of OxFl and OxT compounds as selective fluorescent chemosensors for detecting cobalt and copper ions.

To evaluate and compare the sensitivity of OxFl and OxT to different metal ions, we used the Stern-Volmer (SV) equation (Eq. (1)) to evaluate the fluorescence quenching efficiency [30]. The SV equation describes the quenching data in a homogeneous environment and helps to elucidate the fluorescence quenching mechanism. However, for fluorophores in a heterogeneous environment, the modified Stern-Volmer equation, also known as the Lehrer equation (Eq. (2)), is more applicable [31]. This equation considers the possibility of quenching occurring through two mechanisms simultaneously: a combination of dynamic and static quenching, or the presence of a sphere of action [32].

The Stern-Volmer and Lehrer equations are expressed as follows:

$$I_0/I = 1 + K_{SV}[M^{n+}] \tag{1}$$

$$I_0/(I_0 - I) = 1/f + 1/fK[M^{n+}] \tag{2}$$

In these equations, I_0 and I represent the fluorescence intensities in the absence and presence of the metal ions, respectively, $[M^{n+}] = [Cu^{2+}, Co^{2+}]$ denotes the metal ion concentration, and K_{SV} is the SV quenching constant, which indicates the accessibility of the azomethine molecules to the metal ions. To determine the y-intercept (f^{-1}) and the slope (fK^{-1}), $I_0/(I_0-I)$ was plotted against $1/[M^{n+}]$. The modified SV quenching constant (K = Y-intercept/slope, Table 1) for the accessible population of azomethine molecules interacting with the metal ions can be calculated by dividing the y-intercept (f^{-1}) by the slope (fK^{-1}).

Figures 4A and 5A show that the Stern-Volmer plots for the OxFl and OxT compounds exhibited nonlinear behavior when titrated with Co^{2+} ions. This suggests that the quenching mechanism may involve a combination of static and dynamic processes. To gain a deeper understanding of the interaction mechanism, the experimental data were fitted to the Lehrer equation (a modified form of the SV equation, Eq. (2)), as illustrated in Fig. 4B. However, the SV plots became linear when titrated with Cu^{2+}, as shown in Fig. 4C. When the results in Table 1 were analyzed, it was observed that the K_{SV} constants were greater than those obtained using the Lehrer equation. This observation suggests that the static process plays a more significant role in the quenching mechanism, despite the existence of dynamic quenching [33]. Furthermore, the addition of Cu^{2+} leads to a simpler fluorescence quenching mechanism for both OxFl (Fig. 4C) and OxT azomethines. The K_{SV} value was 1.42×10^4 M^{-1} for OxFl/Co^{2+} and 4.87×10^3 M^{-1} for OxFl/Cu^{2+} as shown in Table 1. These data indicate that the OxFl compound was more sensitive to Co^{2+} ions and had stronger interactions with cobalt ions (Fig. 5).

In conclusion, the use of Stern-Volmer and Lehrer equations allows the distinction between static and

Table 1 LOD, quenching percentage, quenching constant, and binding parameters for interactions of Co^{2+} and Cu^{2+} with OxFl and OxT polyazomethines

Parameters	OxFl		OxT	
	Co^{2+}	Cu^{2+}	Co^{2+}	Cu^{2+}
LOD (M)[a]	3.942×10^{-5}	1.866×10^{-5}	4.598×10^{-5}	2.024×10^{-5}
QP (%)[b]	89.84	64.16	90.08	66.09
Ksv (M^{-1}, Eq. (1))[c]	1.42×10^4	4.87×10^3	1.54×10^4	5.25×10^3
K (M^{-1}, Eq. (2))[d]	7.3×10^3	-	4.45×10^3	-
K_b^{fl}(10^3 M^{-1})[e]	2.01×10^8	2.66×10^3	4.99×10^9	3.76×10^3
ΔG (KJ mol^{-1})	-47.38	-19.54	-55.33	-20.39

[a]*LOD* limit of detection

[b]*QP* quenching percentage (QP = $(I_0$-I)/$I_0 \times 100\%$)

[c]*Ksv* quenching constant calculated with Stern-Volmer (SV) equation

[d]*K* quenching constant calculated with modified SV equation (Lehrer equation)
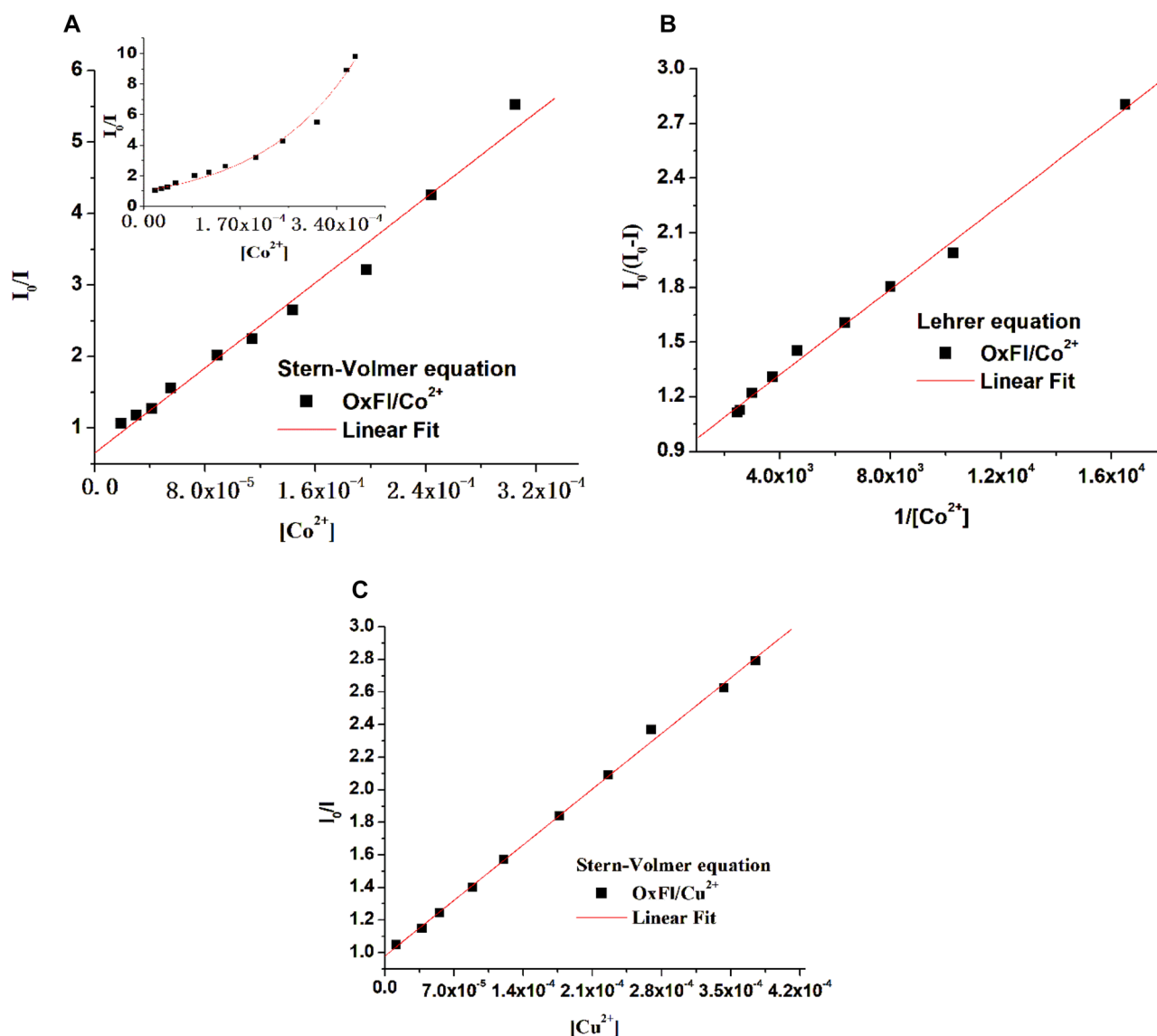
[e]K_b^{fl} Benesi-Hildebrand binding constant

Fig. 4 **A**, **C** Stern-Volmer and **B** modified Stern-Volmer plots (according to the Lehrer equation) for the fluorescence quenching of OxFl by Co^{2+} (**A**, **B**) and Cu^{2+} (**C**) ions. The inset displays the nonlinear plot of the Stern-Volmer curve for OxFl in the range of 0–3.4×10^{-4} mol/L Co^{2+}

dynamic quenching processes. The results revealed that static quenching predominates when interacting with copper ions, while a combination of static and dynamic quenching was observed with cobalt ions. This distinction in quenching behavior highlights the sensitivity of OxFl and OxT compounds to specific metal ions. OxFl is more sensitive to Co^{2+} ions, indicating its potential for selective metal ion detection.

Determination of Binding Parameters

To better understand the binding affinity between OxFl and OxT and the metal ions Co^{2+} and Cu^{2+}, we used the Benesi-Hildebrand relations (Eq. (3) [34, 35]) to calculate the binding constant (K_b^{fl})). The changes in the emission spectra associated with the formation of the respective complexes were analyzed using the following relations:

$$\frac{1}{I_0 - I} = \frac{1}{I_{max} - I_0} + \frac{1}{K_b^{fl}[M^{n+}]\left(I_0 - I_{max}\right)} \tag{3}$$

where $\Delta I = I_0 - I$ represents the change in fluorescence intensity, $\Delta I_{max} = I_{max} - I_0$ denotes the maximum change in fluorescence intensity, $[M^{n+}]$ is the concentration of the metal ion, and K_b^{fl} is the binding constant.
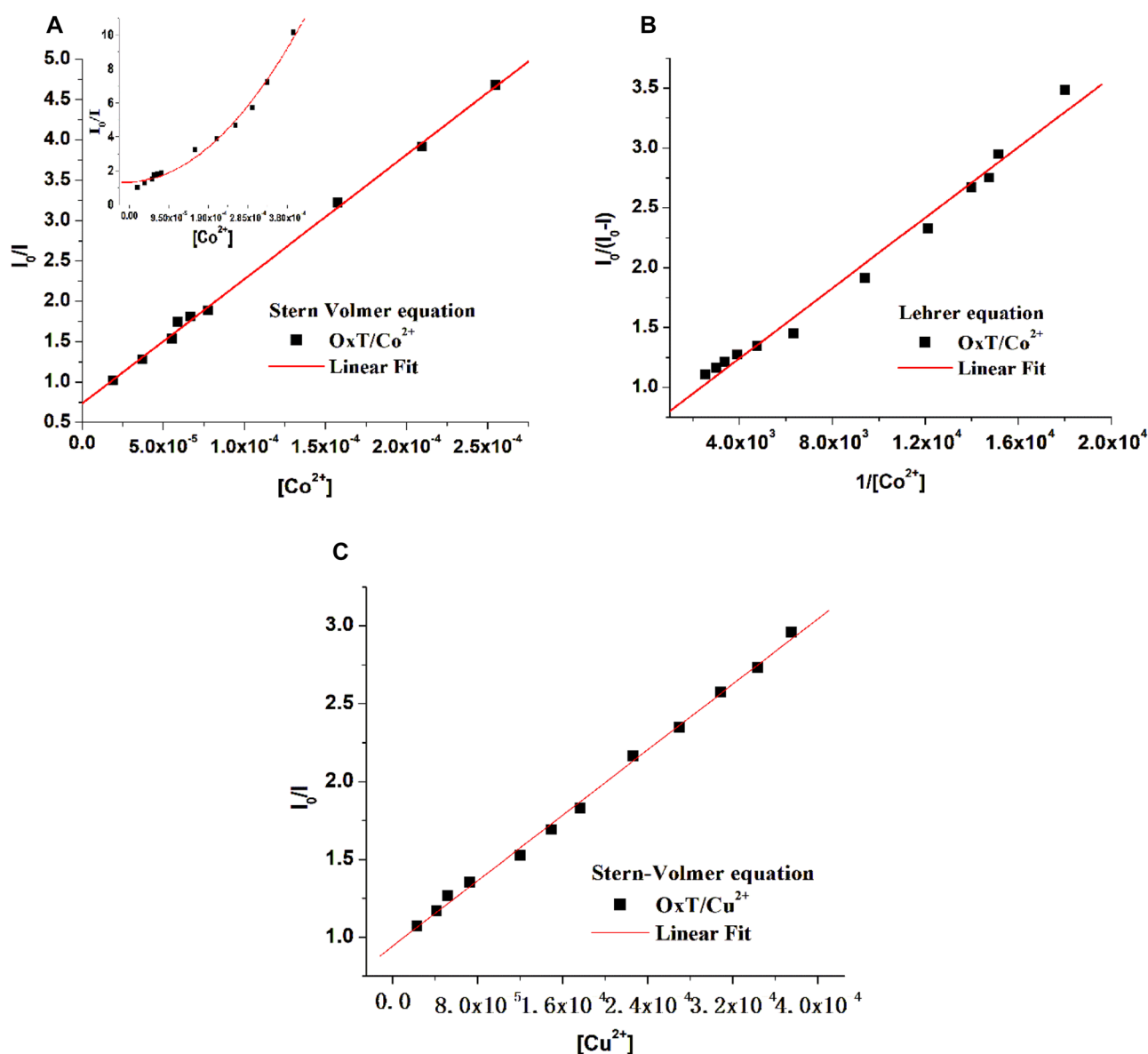
Fig. 5 **A**, **C** Stern-Volmer and **B** modified Stern-Volmer plots (according to Lehrer equation) for the fluorescence quenching of OxT by Co^{2+} (**A**, **B**) and Cu^{2+} (**C**) ions. The inset displays the nonlinear plot of the Stern-Volmer curve for OxT in the range 0–3.8$\times$10^{-4} mol/L Co^{2+}

The binding constants (K_b^{fl}) for OxT and OxFl with Co^{2+} and Cu^{2+} ions were determined by analyzing the plot of 1/I$_0$-I against 1/[Co^{2+}] or 1/[Cu^{2+}] (Fig. 6A–D). The results from Table 1 show that OxT has a higher binding constant of 4.99$\times$10^9 M^{-1}, while OxFl has a lower binding constant of 2.01$\times$10^8 M^{-1} for binding with Co^{2+} ions. This suggests that OxT has a higher binding affinity for cobalt ions than OxFl. The binding

constants indicated that OxFl and OxT bind strongly with Cu^{2+} ions in a 1:1 stoichiometry, as demonstrated by the linear plot of 1/I$_0$-I $vs.$ 1/[Cu^{2+}] (Fig. 6B and D). In contrast, the complexation of Co^{2+} with OxFl and OxT azomethines has a 1:2 binding stoichiometry, confirmed by a polynomial curve, as shown in Fig. 6A and C. Table 1 summarizes the corresponding binding parameters for the fit. The study found that the OxFl and OxT
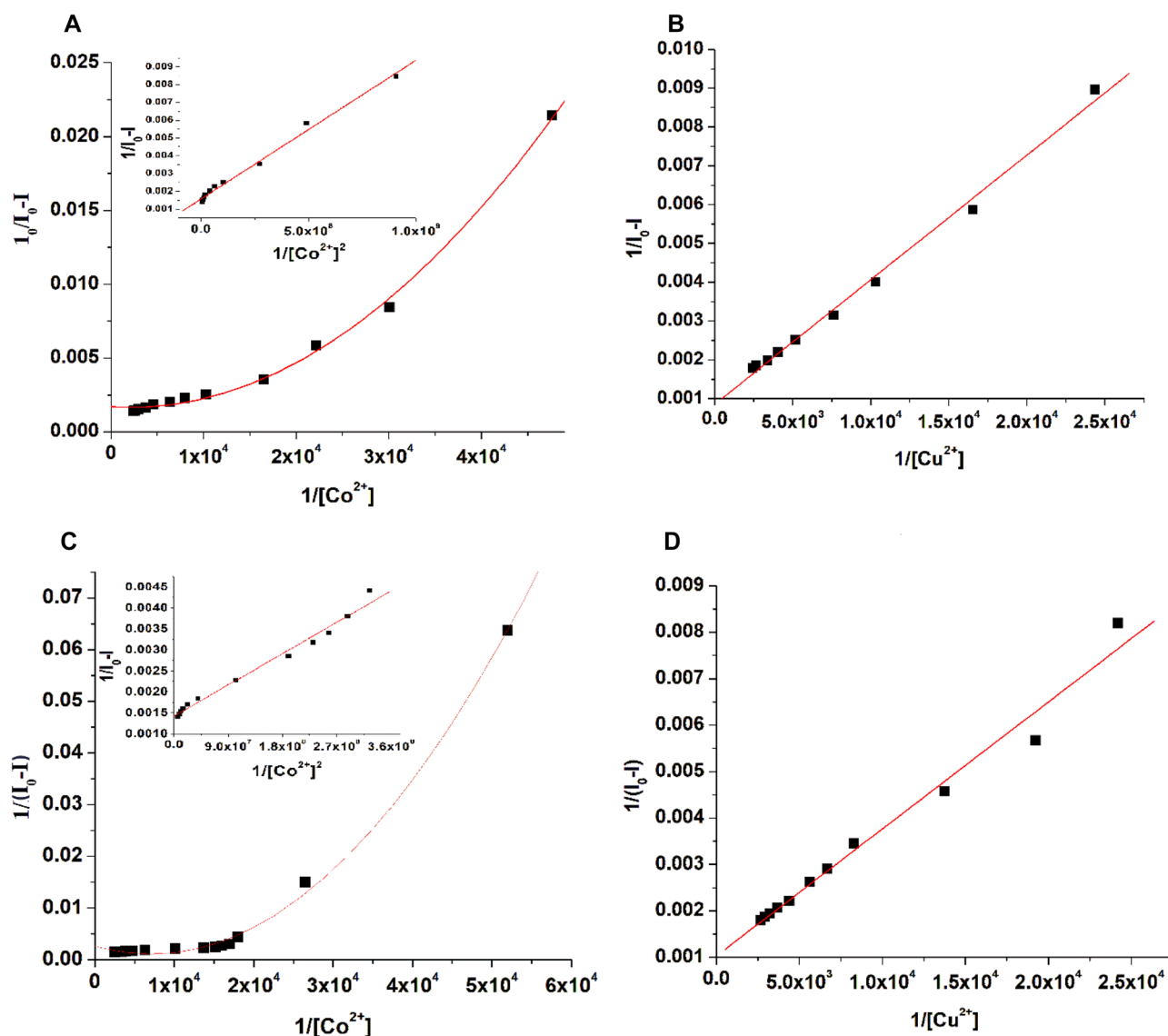
Fig. 6 Benesi-Hildebrand plots for OxFl (**A**, **B**) and OxT (**C**, **D**) compounds with Co^{2+} (**A**, **C**) and Cu^{2+} (**B**, **D**) ions

azomethines have high affinities for Co^{2+} and Cu^{2+} ions, as determined by their binding constants.

The Gibbs free energy (ΔG) values for these processes were estimated using the following equation: $\Delta G = -2.303RT\log K_b^{fl}$ [36], where ΔG (kJ mol^{-1}) represents the free energy change of the complex, R is the universal gas constant (8.314 K^{-1} mol^{-1}), K_b^{fl} (M^{-1}) is the binding constant obtained from the Benesi–Hildebrand

plots and T (273 °C) is the absolute temperature in Kelvin. The calculated ΔG values are listed in Table 1. Negative values indicate that azomethines spontaneously form complexes with Co^{2+} or Cu^{2+} ions at room temperature, confirming their strong binding affinities for these ions.

The findings of this study (Table 1) were compared with the key features of other metal ion detection sensors published in the literature (Table 2).

Table 2 Key features of several metal ion detection sensors from the literature

Metal ion detection sensors	Detection method	Metal ions detected	Sensitivity (limit of detection)	Selectivity	Response time
Benzothiazole azo-derivatives [37]	Multi-sensing (colorimetric, fluorescence)	Cu^{2+} Co^{2+}	Co^{2+} (6.4×10^{-7}M) Cu^{2+} (8.4×10^{-7} M)	Good selectivity for Cu^{2+} and Co^{2+} Moderate (interference from other metal ions)	Rapid color change
Dihydropyridine [38]	Multi-sensing (colorimetric, fluorescence)	Cu^{2+} Co^{2+} Fe^{3+}	Cu^{2+} (1.64 M) Co^{2+} (4.70 M)	Good selectivity for Cu^{2+}, and moderate for Fe^{3+}	Rapid color change
Donor-acceptor chalcone having phenanthrene and thiophene moieties [39]	Multi-sensing (colorimetric, fluorescence)	Co^{2+} Cd^{2+} Pb^{2+} Ni^{2+}	-	Selective for Co^{2+}	-
D-π-A Chalcone Analogue [40]	Fluorescence (turn-on-off-on)	Co^{2+},Fe^{3+} Na^+, K^+	0.15×10^{-3} M	Selective for Co^{2+}	Rapid fluorescence change
2-(2-hydroxyphenyl)-1-H-benzimidazole [41]	Fluorescence	Cu^{2+} Ru^{3+} Ni^{2+}	Cu^{2+} (9.8×10^{-4} mol L^{-1}) Ru^{3+} (7.2×10^{-2} mol L^{-1}) Ni^{2+} (4.5×10^{-3} mol L^{-1})	-	-
Acid Red 94 [42]	-	Pb^{2+} Ag^+	-	Selective for Pb^{2+} and Ag^+	-

Conclusions

In this study, the recognition ability of OxT and OxFl azomethines towards different metal ions in THF solution was investigated using UV-vis absorption and fluorescence spectroscopy. The absorption spectra of these compounds showed two distinct π-π^* transition bands between 273–278 nm and 330–346 nm. OxFl exhibited an additional absorption peak at 309 nm due to the fluorene moiety. The presence of Co^{2+}, Cu^{2+}, Sn^{2+}, and Ni^{2+} ions caused significant spectral changes, indicating the sensitivity of OxT and OxFl azomethines to these ions. Specifically, the fluorescence intensities of these compounds were significantly quenched in the presence of Co^{2+} and Cu^{2+}, indicating their sensitivity to these specific ions. The fluorescence quenching mechanism was analyzed using the Stern-Volmer and Lehrer equations. The results indicate that static quenching was the main mechanism with Cu^{2+} ions, while a combination of static and dynamic quenching was observed with Co^{2+} ions. The binding constants indicate that OxT has a stronger binding affinity for Co^{2+} ions (4.99×10^9 M^{-1}) than OxFl (2.01×10^8 M^{-1}). Both azomethines demonstrated strong binding to Cu^{2+} ions. The negative Gibbs free energy values confirm that the azomethines bind strongly to Co^{2+} or Cu^{2+} ions and spontaneously form complexes at room temperature.

Declarations

Ethical Approval Not applicable.

Competing Interests The authors declare no competing interests.

References

1. Paun A, Hadade ND, Paraschivescu CC, Matache M (2016) J Mat Chem C 4(37):8596
2. Setia S, Sidiq S, De J, Pani I, Pal SK (2016) Liq Cryst 43:2009
3. Han J (2013) J Mat Chem C 1:7779
4. Liu S, Wang Y, Han J (2017) J Photochem Photobiol C 32:78
5. Simon T, Shellaiah M, Srinivasadesikan V, Lin C-C, Ko F-H, Sun KW, Lin M-C (2016) New J Chem 40(7):6101
6. Lin L, Wang D, Chen SH, Wang DJ, Yin GD (2017) Spectrochim Acta Part A Mol Biomol Spectrosc 174:272
7. Tang XL, Peng XH, Dou W, Mao J, Zheng JR, Qin WW, Liu WS, Chang J, Yao XJ (2008) Org Lett 10:3653
8. Zheng CL, Yuan AL, Zhang ZY, Shen H, Bai SY, Wang HB (2013) J Fluoresc 23:785
9. Uriu-Adams JY, Keen CL (2005) Mol Aspects Med 26:268
10. Gaggelli E, Kozlowski H, Valensin D, Valensin G (2006) Chem Rev 106:1995
11. Kumar J, Bhattacharyya PK, Das DK (2015) Spectrochim Acta Part A Mol Biomol Spectrosc 138:99
12. Zhang J, Liu Y, Fei Q, Shan H, Chen F, Liu Q, Chai G, Feng G, Huan Y (2017) Sens Actuators B 239:203
13. Ghaedi M, Niknam K, Taheri K, Hossainian H, Soylak M (2010) Toxicol 48:891
14. Zachariadis GA, Themelis DG, Kosseoglou DJ, Stratis JA (1998) Talanta 47:161
15. Yang X, Wang E (2011) Anal Chem 83:5005
16. Shao X, Gu H, Wang Z, Chai X, Tian Y, Shi G (2013) Anal Chem 85:418
17. Zhu W, Zhang W, Li S, Ma H, Chen W, Panga H (2013) Sens Actuators B 181:773
18. Thangaraj A, Bhardwaj V, Sahoo SK (2019) Photochem Photobiol Sci 18:1533
19. Shi F, Cui S, Liu H, Pu S (2020) Dyes Pigm 173:107914
20. Bhardwaj V, Hindocha L, Kumar SKA, Sahoo SK (2022) New J Chem 46:3248
21. Yüce M, Nazır H, Dönmez G (2010) Bioelectrochemistry 79:66
22. Karami C, Mehr SY, Deymehkar E, Taher MA (2018) Plasmonics 13:537
23. Divya D, Thennarasu S (2021) ChemistrySelect 6(32):8299
24. Wang L, Gong X, Bing Q, Wang G (2018) Microchem J 142:279
25. Hamciuc C, Homocianu M, Hamciuc E (2021) J Mol Liq 336:116268
26. Hamciuc E, Homocianu M, Hamciuc C, Carja I-D (2017) High Perform Polym 30:339
27. Correia FC, Santos TCF, Garcia JR, Peres LO, Wang SHJ (2015) Braz Chem Soc 26:84
28. Slassi S, Aarjane M, Amine A (2021) Appl Organom Chem 35:11
29. Arabahmadi R (2022) J Photochem Photobiol A: Chem 426:113762
30. Papadopoulou A, Green RJ, Frazier RA (2005) J Agric Food Chem 53:158
31. Hare JE, Goodchild SC, Breit SN, Curmi PMG (2016) J Brown Biochemistry 55:3825
32. Lehrer SS (1971) Biochem 10:3254
33. Murariu M, Stroea L (2023) Spectrochim Acta Part A Mol Biomol Spectrosc 291:122279
34. Hu J, Griffith JB, Elioff MS (2023) J Photochem Photobiol A Chem 443:114848
35. Benesi HA, Hildebrand JH (1949) J Am Chem Soc 71:2703
36. Miyan L, Zulkarnain A, Ahmad S (2018) J Mol Liq 262:514
37. El-Nahass MN, Fayed TA, El-Daly HA, Youssif MM (2022) Appl Org Chem 36(6):e6703
38. Hamada WM, El-Nahass MN, Noser AA, Fayed TA, El-Kemary M, Salem MM, Bakr EA (2023) Sci Rep 13(1):15420
39. El-Nahass MN, Fayed TA, Abd Elazim S, El-Gamil MM, Draz DF, Hassan F (2021) J Mol Str 1240:130581
40. El-Nahass MN (2021) J Mol Str 1239:130527
41. El-Sayed YS, Gaber M, El-Nahass MN (2021) J Mol Str 1229:129809
42. Kamel GM, El-Nahass MN, El-Khouly ME, Fayed TA, El-Kemary M (2019) RSC Adv 9(15):8355